

## Studies of ELM Heat Load, SOL Flow and Carbon Erosion from Existing Tokamak Experiments, and Projections for ITER

N. Asakura 1), A. Loarte 2), G. Porter 3), V. Philipps 4), B. Lipschultz 5), A. Kallenbach 6), G. Matthews 7), G. Federici 8), A. Kukushkin 8), A. Mahdavi 9), A.W. Leonard 9), D. Whyte 10), K. Itami 1), H. Takenaga 1), A.V. Chankin 1), S. Higashijima 1), T. Nakano 1), A. Herrmann 6), T. Eich 6), B. LaBombard 5)

- 1) Japan Atomic Energy Research Institute, Naka-machi, Naka-gun, Ibaraki 311-0193, Japan
- 2) EFDA CSU, Max-Planck-Institut für Plasmaphysik, D-85748 Garching bei München, Germany
- 3) Lawrence Livermore National Laboratory P.O.Box 808, Livermore, CA 94550, USA
- 4) Forschungszentrum Jülich, IPP, EURATOM-Association, D-52425 Jülich, Germany
- 5) MIT Plasma Science and Fusion Center, Cambridge, MA 02139, USA
- 6) Max-Planck-Institut für Plasmaphysik, D-85748 Garching bei München, Germany
- 7) Joint European Torus, Abingdon OX13 3EA, Oxon, United Kingdom
- 8) ITER International Team, Max-Planck-Institut für Plasmaphysik, D-85748 Garching bei München, Germany
- 9) General Atomics, P.O.Box 85606, San Diego, CA 92186-5608, USA
- 10) University of California at San Diego, San Diego, CA 92093, USA

e-mail: asakuran@fusion.naka.jaeri.go.jp

**Abstract.** Three important physics issues for the ITER divertor design and operation are summarized based on the experimental and numerical work from multi-machine database (JET, JT-60U, ASDEX Upgrade, DIII-D, Alcator C-Mod and TEXTOR). (i) The energy load associated with Type-I ELMs is of great concern for the lifetime of the ITER divertor target. In order to understand the physics base of the scaling models[1], the ELM heat and particle transport from the edge pedestal to the divertor is investigated. Convective transport during ELMs plays an important role in heat transport to the divertor. (ii) Determination of the SOL flow pattern and the driving mechanism has progressed experimentally and numerically. Influences of the drift effects on the SOL and divertor plasma transport were discussed. (iii) Carbon erosion and redeposition are of great importance in particular for tritium retention via codeposition. Characteristics of chemical yield at two different deposited carbon surfaces, i.e. erosion- and redeposition-dominated areas, have been studied. Progress in the understanding of the chemical erosion is reviewed.

### 1. Introduction

Three important physics issues for the ITER divertor design and operation are summarized based on the experimental and numerical work from multi-machine database (JET, JT-60U, ASDEX Upgrade, DIII-D, Alcator C-Mod and TEXTOR).

- (i) The energy load associated with Type-I ELMs is of great concern for the lifetime of the ITER divertor target. Recently, scaling studies of the normalized ELM energy loss ( $\Delta W_{\text{ELM}}/W_{\text{ped}}$ ) depending on plasma parameters, such as the effective electron collisionality of the pedestal plasma ( $v_{\text{ped}}^*$ ) and pedestal density fraction ( $n_{\text{e,ped}}/n_{\text{GW}}$ ), have progressed[1]. In order to understand the physics base of the scaling models, the ELM heat and particle transport from the edge pedestal to the divertor is investigated [2]. Convective transport during ELMs plays an important role in parallel heat transport and deposition to

the divertor as well as energy loss from the edge in high-density ELMy H-mode plasmas.

- (ii) Control of the divertor plasma and impurity ions is strongly influenced by parallel SOL flow. Determination of the SOL flow pattern and the driving mechanism has progressed experimentally using the Mach probe measurements [3], and numerically using the SOL and divertor simulation code (UEDGE) with including drift effects [4]. Particle flux towards the divertor is influenced by the plasma drifts. Consequences for the divertor plasma characteristics in ITER are discussed.
- (iii) Carbon erosion and redeposition are of great importance, in particular, for tritium retention via codeposition, which is expected to occur during the initial ITER operation with carbon target. Characteristics of chemical yield at two different deposited carbon surfaces, i.e. erosion- and redeposition-dominated areas, have been studied [5]. Progress of quantitative understanding of the chemical erosion is reviewed.

## 2. Studies of SOL Transport and Heat Load Due to Type-I ELM Energy Loss

ELM heat load is determined by plasma transport from the edge pedestal to the divertor as well as ELM energy loss. The role of parallel electron and ion energy transport has been investigated by heat flux measurements with infrared cameras and soft-X-ray emission from hot electrons impinging on the divertor (indicating conductive transport). Electron power pulses evaluated from the soft-X-ray emission in JET have similar duration to edge collapse time by MHD ( $\tau_{MHD}$ ), and it decreases with increasing  $n_{e,ped}$ , which shows that the proportion of energy carried by hot electrons decreases[6]. Therefore, hot electrons play a decreasing role in determining the divertor ELM energy flux with decreasing  $T_{e,ped}$  and increasing  $n_{e,ped}$ .

Energy deposition time from the IR measurements ( $\tau_{IR}^{ELM}$ ) in JET, AUG and JT-60U is well correlated with the characteristic time for ion transport from the pedestal to the divertor,  $\tau_{//}^{Front} = 2\pi R q_{95} / C_{s,ped}$  where  $C_{s,ped}$  is the ion sonic speed calculated from plasma pedestal temperatures, while  $\tau_{MHD}$  remains unchanged ( $\sim 250 \mu s$ ). The good correlation of  $\tau_{IR}^{ELM} [\mu s] = 0.29(\tau_{//}^{Front} [\mu s])^{1.38}$  suggests that convective transport is important for ELM heat deposition to the divertor. The reason of  $\tau_{IR}^{ELM}$  larger than  $\tau_{//}^{Front}$  is probably that the averaged  $T_e$  of the plasma particles expelled with the ELM is lower than  $T_{e,ped}$ , which is used to calculate  $\tau_{//}^{Front}$ .

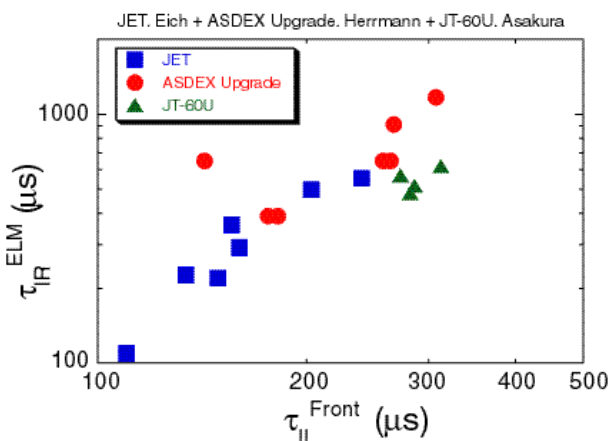


Fig.1 Energy deposition time from IRTV and characteristic time for ion flux to divertor form database (JET, ASDEX-U, JT-60U)

In JT-60U,  $\tau_{IR}$  (250-350 $\mu s$ ) is comparable to the duration of ELM-enhanced ion flux and the SOL flow velocity (i.e. Mach number increases to ion sonic level) measured with Mach probe just below the X-point [7]. The convective heat flux,  $\gamma_{//} [5/2kT_i + 5/2kT_e + 1/2m_i(MC_s)^2] \sin\theta_{div}$  where  $\gamma_{//}$  and  $\theta_{div}$  are the ion flux and the field line pitch angle on divertor plate, reaches up to

70-80% of the total heat flux measured by IRTV, provided that the ELM-enhanced particle flux has  $T_e$ ,  $T_i$  and  $C_s$  measured at the pedestal. This is in agreement with the good correlation found between  $\tau_{IR}^{ELM}$  and  $\tau_{//}^{Front}$ . The fraction of convective heat flux would be comparable to or smaller than conductive heat flux, if  $T_e$ ,  $T_i$  and  $C_s$  for the averaged exhausted plasma are used.

Above progress in the SOL transport study provides a good physics basis on which to extrapolate present experimental results of Type-1 ELM energy losses to ITER. An interpretation of  $\Delta W_{ELM}/W_{ped}$  database as a function of  $v_{ped}^*$  (based on MHD instability models produced by edge bootstrap current) suggested unacceptable value of  $\Delta W_{ELM}/W_{ped} = 0.15-0.2$  for ITER ( $v_{ped}^* \sim 0.03$ ). On the other hand,  $\Delta W_{ELM}/W_{ped}$  is small (0.1-0.15[8] and 0.05-0.1[2]) for the models based on the SOL convective transport, which would be allowable for ITER divertor lifetime for an inclined target option [9]. Determination of conductive and convective processes in the SOL is crucial for quantitative evaluation of the ELM energy loss.

### 3. Plasma Flow and Effects of the Plasma Drifts in SOL and Divertor

Poloidal variation of the parallel SOL flow, i.e. at high-field-side (HFS), low-field-side (LFS), plasma top SOLs and the private flux region, were determined using reciprocating Mach probes (JT-60U, JET, Alcator C-mod, DIII-D and AUG), which demonstrated a consistent picture: net particle fluxes to the LFS and HFS divertors, but the SOL flow from the LFS SOL to the HFS divertor through the plasma top for the ion  $\nabla B$  drift direction towards the divertor. At the same time, in the private flux region, drift flow to the HFS divertor is produced by large  $E_r \times B$  drift [10]. Particle fluxes towards the HFS divertor are experimentally investigated with increasing  $\bar{n}_e$  in JT-60U[3] as shown in Fig.2, where  $n^{GW} = 5.2 \times 10^{19} m^{-3}$ . Drift flux ( $\Gamma_{p,drift}^{HFS}$ ) is away from the HFS divertor, and its fraction decreases from 50% to 10% with increasing  $\bar{n}_e$ . Thus, net particle flux ( $\Gamma_p^{HFS}$ ) is always towards the HFS divertor. On the other hand, the drift flux in the private region ( $\Gamma_p^{Prv}$ ) is comparable to or larger than  $\Gamma_p^{HFS}$  under the attached divertor condition. HFS-enhanced asymmetry in divertor ion flux is produced mainly by  $\Gamma_p^{Prv}$ .

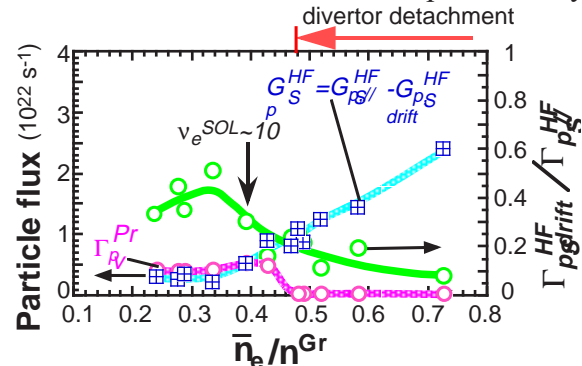


Fig.2 Particle fluxes towards HFS divertor,  $\Gamma_{p,drift}^{HFS}$  and  $\Gamma_p^{Prv}$ , and ratio of drift flux,  $\Gamma_{p,drift}^{HFS}/\Gamma_p^{HFS}$  as a function of  $n_e$ , where the ion grad-B drift direction is towards divertor.

Various mechanisms producing the parallel SOL plasma flow such as  $E \times B$ ,  $B \times \nabla B$  and diamagnetic drifts were recently discussed. The numerical approach to understand the SOL flow pattern has progressed using the UEDGE code with the drift effects included [11]. Results for a JT-60U L-mode case [4] show that the SOL flow is produced from LFS midplane to HFS divertor, which is caused mainly by ion  $B \times \nabla B$  drift. Mach numbers of the SOL flow are 0.1-0.2 at LFS and increase from 0.2 to 0.6 at HFS with  $\bar{n}_e$  (as shown in Fig.3), which are smaller than and comparable to the measurements at  $\bar{n}_e = 1.5 \times 10^{19} m^{-3}$  (0.3-0.4 and  $\sim 0.4$ ), respectively. Simulation of H-mode plasmas suggests that the effect of drifts becomes more important in H-mode as the radial temperature gradient scale length is smaller, and that the existence of large parallel pressure gradient drives fast flow.

Simulation also suggests large carbon ion flow in the private flux region similar to the plasma drift flow, which may lead to accumulation of carbon on HFS divertor plate.

Although high density core plasma ( $\bar{n}_e/n^{GW} \sim 0.85$ ) is sustained in ITER, electron collisionality of the SOL plasma is relatively low ( $v_e^{SOL} = L_{cl}/\lambda_{ee} \sim 5-10$ ) since  $T_e$  at separatrix ( $\sim 150$  eV) would be high where  $n_e \sim 3.5 \times 10^{19} \text{ m}^{-3}$ . Relatively large  $E_r$  is expected in such low  $v_e^{SOL}$ , which corresponds to database at  $\bar{n}_e/n^{GW} \sim 0.4$  in Fig.2, and  $\Gamma_{p,drift}^{HFS}/\Gamma_{p,||}^{HFS}$  of  $\sim 30\%$  would be anticipated. At the same time, the  $E_r \times B$  drift flow in the private flux region is expected just below the X-point since the detachment is localized near the strike-points. Particle flux towards the divertor would be influenced by these drifts, and a design work including the drift effects will be useful to optimize the divertor and pump geometries.

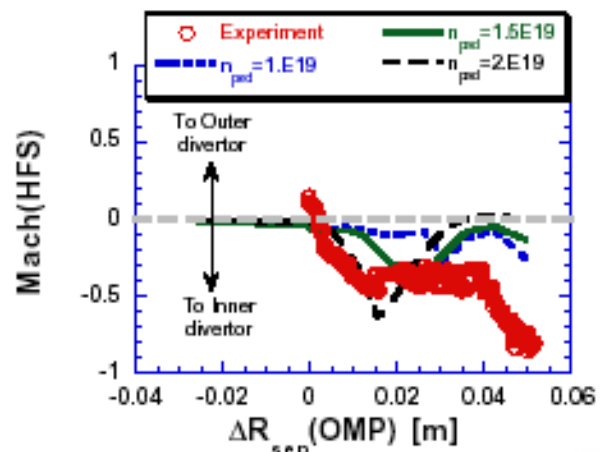


Fig. 3 Profiles of Mach numbers at HFS SOL (above HFS baffle): measurement (circles,  $n_e = 1.5 \times 10^{19} \text{ m}^{-3}$ ) and simulations for three  $n_e$  scan.

#### 4. Chemical Erosion Under Fusion Relevant Condition

Over the last two years many tokamaks and laboratory experiments have been carried out to better characterize the chemical erosion yield of carbon for ion flux density of  $10^{21}-10^{23} \text{ m}^{-2}\text{s}^{-1}$  and low impact energies. However, there are several aspects of erosion/redeposition that are uncertain and require further investigation in current machines in order to extrapolate reliably to ITER. One particular complication arises from differences in chemical erosion yields between areas of net erosion and net re-deposition; the structure of the re-deposited carbon films (containing hydrogen isotope) also depends on the energies of the incident ions and neutrals [5].

On the re-deposition dominated areas, carbon can be deposited in the form of soft layers, and re-erosion proceeds due to atomic and low energy ion fluxes. This is observed for example in the JET HFS divertor, which is routinely detached and exposed to high density and low energy hydrogen atoms and molecules. In this process, contribution of higher hydrocarbons to the total sputtered carbon atoms was found to dominate (i.e. half of the total methane). Large contribution ( $\sim 80\%$ ) from higher hydrocarbons was also found in simultaneous CD and  $C_2$  measurements of JT-60U LFS divertor [12] (where net erosion dominated) at surface temperature,  $T_{surf}$ , of 440 and 560K. Overall chemical yields are large between 7 and 20% for the two tokamaks, and large influence of  $T_{surf}$  on the chemical yields was observed. Thus, contributions of higher hydrocarbons and generation conditions should be clarified in order to infer chemical yield under the higher flux density

On the net-erosion dominated areas (mostly in the LFS divertor of most devices), overall trends indicate that chemical yields between 3-5 % are a good guess. There are weak indications of flux dependence for JET[13] and TEXTOR(limiter)[14] up to flux density of  $5-10 \times 10^{22} \text{ m}^{-2}\text{s}^{-1}$  as shown in Fig.4. At the same time, most data show a weak dependence on

$T_{\text{suf}}$  (in 400-600K). Here, methane-originated chemical yields are plotted for JT-60U due to large contribution from higher hydrocarbons compared to those in other tokamaks. The yields slightly decrease at high flux ( $\Gamma^{-\alpha}$ ,  $\alpha=0.1\sim 0.4$ ) and  $T_{\text{suf}}$  dependence is larger than other tokamaks. Yields for ASDEX-U decreased to  $\sim 1\%$  as  $\Gamma^{-\alpha}$ ,  $\alpha\sim 0.7$  [15], and very low chemical yields (lower than 0.3-0.5%) was reported in DIII-D long-exposed tiles [16].

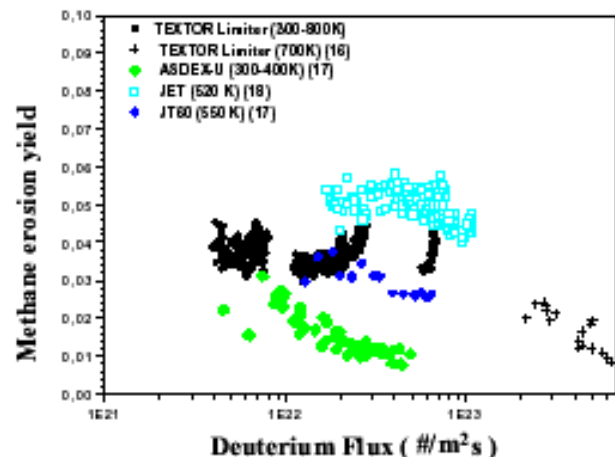


Fig. 4 Chemical erosion yields of Methane as a function of ion flux density.

To date no definitive conclusion can be drawn on carbon chemical erosion yields at high flux density in ITER (several  $10^{23} \text{ m}^{-2}\text{s}^{-1}$ ). More experiments are needed to better determine the extent to which parameters other than flux (e.g., energy, re-deposition, photon efficiency and viewing geometry in spectroscopic measurements, yields of higher hydrocarbons etc.) affect the observed erosion rates in current machines.

## 5. Conclusions

Understanding of important physics issues for the ITER divertor design and operation, (i) divertor heat load associated with Type-I ELMs, (ii) parallel SOL plasma transport produced by the SOL flow and drift flow, have been progressed based on the experimental and numerical work from multi-machine database. (iii) There has been some progress in the characterization of chemical erosion yields in C-clad divertor tokamaks. In order to make reliable extrapolation for ITER, the R&D program needs to better address the physics of the erosion mechanisms and the transportation and redeposition of eroded material and resulting mixing effects.

## References

- [1] LOARTE, A., et al., "Predicted ELM energy loss and power loading in ITER-FEAT", Fusion Energy 2000 (Proc. 18<sup>th</sup> Int. Conf. Sorrento, 2000), IAEA, Vienna (2001) (CD-ROM file ITERP/11).
- [2] LOARTE, A., et al., "ELM energy and particle losses and their extrapolation to burning plasma experiments", PSI 2002, accepted to J. Nucl. Mater.
- [3] ASAKURA, N., et al., "Plasma flow measurement in high- and low-field-side SOL and influence on the divertor plasma in JT-60U tokamak", PSI 2002, accepted to J. Nucl. Mater.
- [4] PORTER, G., et al., "Simulation of the effect of plasma flows in DIII-D, JET, and JT-60U", PSI 2002, accepted to J. Nucl. Mater.
- [5] PHILIPPS, V., et al., "Chemical erosion behavior of carbon materials in fusion devices", PSI 2002, accepted to J. Nucl. Mater.
- [6] LOARTE, A., et al., Plasma Phys. Control. Fusion **44** (2002) 1815.
- [7] ASAKURA, N., et al. Plasma Phys. Control. Fusion **44** (2002) A313.
- [8] JANESCHITZ, G., et al., J. Nucl. Mater. **290-293** (2001) 1.
- [9] FEDERICI, J., et al., "Key ITER plasma edge and plasma-material interaction issues", PSI 2002, accepted to J. Nucl. Mater.
- [10] BOEDO, J.A., et al., Phys. Plasma **7** (2000) 1075.
- [11] PORTER, G.D., et al., Phys. Plasma **7** (2000) 3663.
- [12] NAKANO, T., et al., Nucl. Fusion **42** (2002) 689.
- [13] STAMP, M.F., et al., J. Nucl. Mater. **290-293** (2001) 321.
- [14] POSPIESZCZYK, A., et al., J. Nucl. Mater. **241-243** (1997) 833.
- [15] KALLENBACH, A., et al., J. Nucl. Mater. **266-269** (1999) 243.
- [16] WHYTE, D.G., et al., J. Nucl. Mater. **290-293** (2001) 356.